IEEE Access
Multidisciplinary ⋮ Rapid Review ⋮ Open Access Journal

Received January 5, 2021, accepted January 12, 2021, date of publication January 18, 2021, date of current version January 25, 2021.

Digital Object Identifier 10.1109/ACCESS.2021.3052153

Gradient-Based Optimizer for Parameter Extraction in Photovoltaic Models

ALAA A. K. ISMAEEL[1,2], ESSAM H. HOUSSEIN[3], DIEGO OLIVA[4,5], AND MOKHTAR SAID[6]

[1]Faculty of Computer Studies (FCS), Arab Open University (AOU), Muscat 130, Oman
[2]Faculty of Science, Minia University, Minia 61519, Egypt
[3]Faculty of Computers and Information, Minia University, Minia 61519, Egypt
[4]IN3–Computer Science Department, Universitat Oberta de Catalunya, 08860 Castelldefels, Spain
[5]Departamento de Ciencias Computacionales, Universidad de Guadalajara, CUCEI, Guadalajara 44430, Mexico
[6]Electrical Engineering Department, Faculty of Engineering, Fayoum University, Faiyum 63514, Egypt

Corresponding author: Alaa A. K. Ismaeel (alaa.ismaeel@aou.edu.om)

ABSTRACT Solar radiation is increasingly used as a clean energy source, and photovoltaic (PV) panels that contain solar cells (SCs) transform solar energy into electricity. The current-voltage characteristics for PV models is nonlinear. Due to a lack of data on the manufacturer's datasheet for PV models, there are several unknown parameters. It is necessary to accurately design the PV systems by defining the intrinsic parameters of the SCs. Various methods have been proposed to estimate the unknown parameters of PV cells. However, their results are often inaccurate. In this article, a gradient-based optimizer (GBO) was applied as an efficient and accurate methodology to estimate the parameters of SCs and PV modules. Three common SC models, namely, single-diode models (SDMs), double-diode models (DDMs), and three-diode models (TDMs) were used to demonstrate the capacity of the GBO to estimate the parameters of SCs. The proposed GBO algorithm for estimating the optimal values of the parameters for various SCs models are applied on the real data of a 55 mm diameter commercial R.T.C-France SC. Comparison between the GBO and other algorithms are performed for the same data set. The smallest value of the error between the experimental and the simulated data is achieved by the proposed GBO. Also, high closeness between the simulated P-V and I-V curves is achieved by the proposed GBO compared with the experimental.

INDEX TERMS Gradient-based optimizer, photovoltaic modules, diode models, renewable energy, solar energy.

I. INTRODUCTION

Human life is stable due to energy, and improving life requires the development and progress of energy. As conventional sources of energy are depleted, they cause environmental exacerbation. Considering the above, the dependence on renewable energy sources is inevitable because it is clean, reduces environmental problems, exists in abundance, and has a variety of uses [1]–[3].

The main types of renewable energy sources are solar energy, wind energy, etc. Recently, a huge improvement in the performance of energy generated from these sources has been developed [4]–[6]. The use of clean and renewable energy sources is one of the most point in the research study [7]. One of the main renewable energy sources is the solar PV technology, that is used in several applications such as satellites [8], water desalination [9], cooling and heating [10]. So that the accurate modeling and simulation of solar cell is performed with several techniques such as adaptive control [11], [12] and numerical simulation [13]. The maintenance of SC panels is required [14].

SCs are constructed with semiconductor material of P-N junction that has a quasi-neutral region, space-charge region, and defect region. The losses in this region are due to the recombination and diffusion of the charge transporter. These losses must be considered in the development of the PV model. A photo-generated current is expressed in the ideal model of a PV cell. The value of the current generated from a real PV model veers about the experimental value due to losses in the semiconductor P-N junction. This leads to the establishment of the PV model in SDMs [15]. This model is simple and fast. Furthermore, the quasi-neutral region losses can be expressed into the SDM. Meanwhile, a DDM was applied to achieve higher accuracy. The DDM presents the losses expressed in the SDM and the space charge region losses. Meanwhile, a TDM was applied to achieve more

The associate editor coordinating the review of this manuscript and approving it for publication was Dipankar Deb.

accuracy than the SDMs and DDMs. The losses expressed by the TDM were defect region losses and the ones described in the DDM [16].

To properly model the behavior of the PV modules, the diode representations possessed some parameters that could affect their output. They needed to be calibrated according to the information used in the design. There are five unknown parameters in SDMs, seven in DDMs, and nine in TDMs. These parameters are commonly estimated in two ways: by using metaheuristic optimization algorithms [17] and with iterative mathematical methods [18]. These parameters are estimated from multiple approaches, such as the iterative mathematical techniques that estimate five parameters by assuming the value of the ideality factor [18]. Also, the Lambert W-function method was applied to estimate these parameters from the datasheet of PV cells [19], [20]. The least squares method and the Gauss-Seidel method were used as an iterative approach in the parameter's extraction [21]–[24]. The complex and nonlinear optimization problem derived from the identification of internal parameters was solved with metaheuristic algorithms. This is possible due to the improvement of swarm intelligence and the development of computers [25].

Due to the nonlinearity behavior of photovoltaic models and increasing number of parameters required to be estimated, the metaheuristic algorithms are applied to achieve high accuracy for the extracted parameters. Several optimization techniques have been used for the extraction and estimation of PV parameters. The multiple learning backtracking search algorithm (MLBSA) was developed to estimate PV parameters with high accuracy and reliability in [26], in which the grey wolf optimizer (GWO) and the cuckoo search algorithm (CSA) were combined in a method called GWOCS to extract these parameters with the aim of achieving an appropriate balance between the exploration and exploitation in [27], and an opposition-based sine cosine approach with local search was used to identify the optimal parameters. This optimizer design was based on the exploratory and exploitative cores of the sine cosine algorithm (SCA) [28]. The parameters of PV cells were also identified using a logistic chaotic JAYA algorithm (LCJAYA) with high performance [29]. In the same context, the winner-leading competitive swarm optimizer with dynamic gaussian mutation [30] and coyote optimization algorithm (COA) [31] are applied for extracting the photovoltaic parameters.

The seven unknown parameters in the DDM were extracted with different optimization techniques like the moth flame algorithm and the orthogonal nelder-mead moth flame optimization (NM-SOLMFO), which were applied to increase the accuracy and reliability of the optimization process in [32]. PV parameters were also identified by using the teaching learning-based and the improved teaching learning-based optimization algorithm (ITLBO) with high reliability and accuracy [33]. On the other hand, for TDM, some researchers assumed the value of the ideality-factor for the second and third diodes [34]. Then the parameters were estimated with methods like the interval branch and the bound global optimization algorithm [35]. Also, the simplified teaching learning-based optimization (STBLO) was applied to estimate the parameters in TDM [36]. Parameter extraction was prepared by an improved version of the whale optimization algorithm using the opposition-based learning (OBWOA) [37], the chaotic improved artificial bee colony (CIABC) [38], and Harris hawk optimization (HHO) [39].

In the related literature, several metaheuristic optimization algorithms have been applied to extract the PV parameters such as the traditional genetic algorithm (GA) and its improvements [40]–[42], the differential evolution with its generation [43]–[45], the artificial bee swarm algorithms [46], the improved ant lion algorithm [47], the salp swarm-inspired algorithm [48], [49], the bio-geography based optimization [50], the improved cuckoo search algorithm [51], the bird mating optimization [52], the hybrid bee pollinator flower pollination algorithm [53], the bacterial foraging algorithm [54] and the artificial immune system [55]. To estimate the parameter of SDMs, different approaches have been used like the boosted mutation-based Harris hawks optimizer [56], the improved electromagnetic-like algorithm [57], the grasshopper optimization algorithm [58], the improved whale optimization algorithm [59], and the shark smell optimizer [60].

MOTIVATION AND CONTRIBUTIONS

Logically, No Free Lunch (NFL) theorem [61] has proved that there is no metaheuristic optimization technique for solving all optimization problems. According to this theorem, the superior performance of an optimizer on a class of problems cannot guarantee the similar performance on another class of problems. This theorem is the foundation of many work in the literature and allows researchers in this field to adapt the current techniques for new classes of problems. The purpose of this study is to propose an efficient search mechanism for estimating the unknown parameters of PV cells. In this study, a gradient-based optimizer (GBO) was applied to estimate the parameters of the three common SC models, namely, single-diode model (SDM), double-diode model (DDM), and three-diode model (TDM). The GBO algorithm shows a strong performance of parameter optimization, which has be proved in [62]. The GBO algorithm has various advantages, such as solution accuracy, balance, convergence speed, between analysis and exploitation and also shows a strong performance of parameter optimization, which has be proved in [62]. This is the foundation and motivation of this work as well, in which we apply GBO to solve this problem.

To summarize, the major contributions of this work are:

- The parameters of three models of PV cells were estimated with a new GBO to minimize the objective function.
- The validation of the GBO algorithm was performed by changing the PV models (SDM, DDM, and TDM).

- The parameters extracted from previous works and another two optimization algorithms were used for comparison with the proposed GBO algorithm over the same data set of R.T.C France solar cells.
- Statistical analysis was used to study the performance of the proposed GBO technique compared with other algorithms.
- The efficiency of the proposed GBO was verified by checking the value of absolute error of the current and power at the best root mean square.
- The P-V and I-V curves were simulated for the estimated parameters values to graphically verify the accuracy of the proposal.

The organization of this paper is as follows: Section II discusses the analysis of PV diode models, Section III explains the objective function, Section IV presents an overview for the GBO, the simulation and results are discussed in V, and the conclusion of this paper is illustrated in Section VI.

II. ANALYSIS OF PV MODELS

Three PV models are analyzed in this section: SDMs, DDMs, and TDMs. They are electrical circuits that will be described in detail in the following subsections.

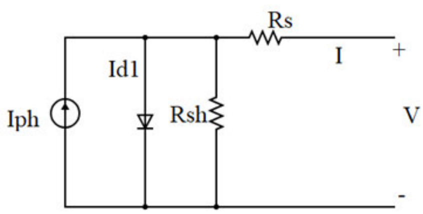

FIGURE 1. Equivalent circuit of the SDM.

A. ANALYSIS OF THE SINGLE DIODE MODEL

The equivalent circuit of the SDM is described in Figure 1. It contains only one diode that permits the shunting of the photogenerated current I_{ph}. In the SDM, the total current was computed by using the following equation:

$$I = I_{ph} - I_{d1} - I_{sh} \tag{1}$$

where, I is the total current, I_{ph} corresponds to the photogenerated current, I_{d1} is the diode current and I_{sh} is the shunt resistor current. Since the diode was constructed from semiconductor materials, some internal parameters can be manipulated to increase the quality of the output values. The Shockley diode equation helped to handle the intrinsic values of the diode. Considering this fact, Eq.(1) is rewritten as:

$$I = I_{ph} - I_{s1}\left(e^{\frac{q(V+IR_s)}{a_1 kT_c}} - 1\right) - \left(\frac{V+IR_s}{R_{sh}}\right) \tag{2}$$

In Eq.(2), V is the total voltage, I_{s1} is the diode reverse saturation current, R_{sh} is the shunt resistance, R_s is the series resistance. a_1 is the non-physical ideality factor, $k = 1.3806503 \times 10^{-23}(J/K)$ is the Boltzmann's constant, the variable $q = 1.60217646 \times 10^{-19} C$ is the charge of the electron, finally T_c is the temperature in Kelvin. The efficiency of the model is provided by the outputs V and I and the unknown parameters of the SDM are (I_{ph}, I_{s1}, a_1, R_s, and R_{sh}). As is expected, a proper configuration of such a parameter will directly affect the output.

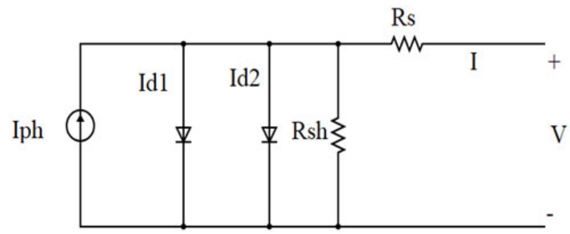

FIGURE 2. DDM equivalent circuit.

B. ANALYSIS OF THE DOUBLE DIODE MODEL

Another interpretation of the PV modules is the DDM. Its equivalent circuit is described in Figure 2. The advantage of a DDM is that it considers the loss of recombination currents in the depletion region. Notice that the SDM does not include this information. The total current of the DDM is computed as follows:

$$I = I_{ph} - I_{d1} - I_{d2} - I_{sh} \tag{3}$$

By using the Shockley function the Eq.(3) can be rewritten as:

$$\begin{aligned} I = I_{ph} &- I_{s1}\left(e^{\frac{q(V+IR_s)}{a_1 kT_c}} - 1\right) \\ &- I_{s2}\left(e^{\frac{q(V+IR_s)}{a_2 kT_c}} - 1\right) \\ &- \left(\frac{V+IR_s}{R_{sh}}\right) \end{aligned} \tag{4}$$

In Eq.(4), I_{d2} is the saturation current for the second diode. a_2 is the second diode ideality factor. As opposed to the SDM, the DDM has seven parameters that must be estimated and they are (I_{ph}, I_{s1}, a_1, R_s, R_{sh}, I_{s2}, and a_2).

C. ANALYSIS OF THE THREE DIODE MODEL

In the TDM, an extra diode is added to the DDM to consider and simulate the leakage current in the grain boundaries that are present in commercial CSs [63], [64]. The TDM equivalent circuit is described in Figure 3 and the total current is computed as:

$$I = I_{ph} - I_{d1} - I_{d2} - I_{d3} - I_{sh} \tag{5}$$

In Eq.(5) the Shockley function is replace for each diode. Then the result is the following equation:

$$\begin{aligned} I = I_{ph} &- I_{s1}\left(e^{\frac{q(V+IR_s)}{a_1 KT_c}} - 1\right) \\ &- I_{s2}\left(e^{\frac{q(V+IR_s)}{a_2 KT_c}} - 1\right) \\ &- I_{s3}\left(e^{\frac{q(V+IR_s)}{a_3 KT_c}} - 1\right) \\ &- \left(\frac{V+IR_s}{R_{sh}}\right) \end{aligned} \tag{6}$$

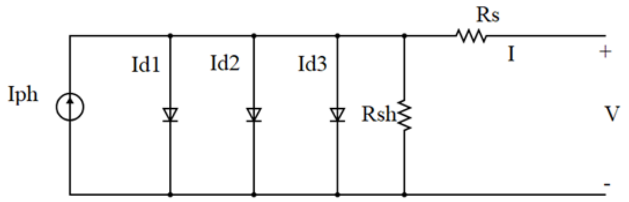

FIGURE 3. TDM equivalent circuit.

In Eq.(6), a_3 is the third diode ideality factor, while I_{d3} is the third diode saturation current. Notice that the inclusion of a third diode also increases the number of parameter that must be properly estimated. The nine parameters are ($I_{ph}, I_{s1}, a_1, R_s, R_{sh}, I_{s2}, a_2, I_{s3}$, and a_3).

III. THE OBJECTIVE FUNCTION FOR PHOTOVOLTAIC PARAMETER ESTIMATION

The optimization algorithms are used to extract the parameters of different models of PV cells. These techniques need an objective function that permits the evaluation of the candidate solutions. The optimization problems are defined in bounded spaces. These boundaries are defined in Table 1.

TABLE 1. The boundaries of extracted photovoltaic parameters [26].

Parameters	Lower bound	Upper bound
$I_{ph}(A)$	0	1
$I_{s1}, I_{s2}, I_{s3}(\mu A)$	0	1
$R_s(\Omega)$	0	0.5
$R_{sh}(\Omega)$	0	100
a_1, a_2, a_3	1	2

The root mean square error (RMSE) is the objective function and must be minimized by the optimizer technique. The X decision variables are extracted each time the optimizer is run. The mathematical formula to compute RMSE is defined as follows:

$$J(V, I, X) = I - I_{exp} \tag{7}$$

The vector of decision variables for the SDM is $X = (I_{ph}, I_{s1}, a_1, R_s, R_{sh})$. The vector of decision variables for the DDM is $X = (I_{ph}, I_{s1}, a_1, R_s, R_{sh}, I_{s2}, a_2)$. The vector of decision variables for the TDM is $X = (I_{ph}, I_{s1}, a_1, R_s, R_{sh}, I_{s2}, a_2, I_{s3}, a_3)$.

$$RMSE = \sqrt{1/N \sum_{i=1}^{N} (J(V, I, X))^2} \tag{8}$$

where I_{exp} is the experimental current and N is the reading data number.

IV. GRADIENT-BASED OPTIMIZER

A GBO [62] is based on the idea of the integration of population-based methods with a gradient technique to solve complex optimization problems. The GBO algorithm utilizes Newton's method to control the search agent's direction while exploring the problem space. The GBO algorithm has two basic components, including the gradient search rule and the locale escaping operator.

A. INITIALIZATION STAGE

Like most metaheuristic algorithms, the GBO starts the optimization process with an initial population generated independently from uniform random distribution. Each population agent is called a "vector", and the population has a number of N vector agents in a D-dimensional search space. The initialization process is then performed as follows:

$$X_n = X_{min} + rand(0, 1) \times (X_{max} - X_{min}) \tag{9}$$

where X_{min}, and X_{max} are the bounds of decision variables X, and $rand(0, 1)$ is a random number defined in the range [0, 1].

B. GRADIENT SEARCH RULE STAGE

As mentioned previously, the GBO algorithm begins with a random set of initial solutions and updates each agent position depending on a gradient specified direction. To guarantee balance between exploration of significant search space regions and exploitation to reach near optimum and global points, a significant factor ρ_1 is employed as follows:

$$\rho_1 = 2 \times \text{rand} \times \alpha - \alpha \tag{10}$$

$$\alpha = \left| \beta \times \sin\left(\frac{3\pi}{2} + \sin\left(\beta \times \frac{3\pi}{2}\right)\right) \right| \tag{11}$$

$$\beta = \beta_{\min} + (\beta_{\max} - \beta_{\min}) \times \left(1 - \left(\frac{m}{M}\right)^3\right)^2 \tag{12}$$

where $\beta_{\min}$ and $\beta_{\max}$ are constant values 0.2 and 1.2, respectively, m represents the current iteration number, while M represents the total number of iterations. To balance the exploration and exploitation processes, the parameter ρ_1 changes based on the sine function α. This parameter value changes throughout the iterations. It starts with a large value through the first optimization iterations in order to improve population diversity. Then, the value decreases throughout iterations to accelerate population convergence. The parameter value increases throughout defined iterations within a range [550, 750], which in turn increases solution diversity and converges around the best obtained solution and the exploration of more solutions. Therefore, an algorithm is enabled to avoid local sub-regions. Thus, GSR can be determined as follows:

$$GSR = randn \times \rho_1 \times \frac{2\Delta x \times x_n}{(x_{\text{worst}} - x_{best} + \varepsilon)} \tag{13}$$

The concept of GSR provides the GBO algorithm with random behavior across iterations, therefore, strengthening exploration behavior and escaping from local optima. In Eq.(13), the factor Δx is defined and measures the difference between the best solution (x_{best}) and a randomly selected solution x_{r1}^m. To ensure that Δx changes through iterations, the parameter δ is computed by Eq.(16). Additionally, to improve exploration, a random number (randn) is added to this equation.

$$\Delta x = \text{rand}(1:N) \times |\,\text{step}\,| \tag{14}$$

$$\text{step} = \frac{\left(x_{\text{best}} - x_{r1}^m\right) + \delta}{2} \tag{15}$$

$$\delta = 2 \times \text{rand} \times \left(\left| \frac{x_{r1}^m + x_{r2}^m + x_{r3}^m + x_{r4}^m}{4} - x_n^m \right| \right) \tag{16}$$

where $rand(1:N)$ is a vector of N random values $\in [0, 1]$. $r1, r2, r3$, and $r4$ are different integers randomly chosen from [1, N] such that $(r1 \neq r2 \neq r3 \neq r4 \neq n)$. *step* represents a step size, which is determined by x_{best} and x_{r1}^m.

The direction of movement (DM) is employed to converge around the area of solution x_n. This term uses the best vector and moves the current vector (x_n) in the direction of $(x_{best} - x_n)$. This process provide a convenient local search tendency with a significant affect on GBO convergence. The DM is computed with the following formula:

$$DM = rand \times \rho_2 \times (x_{best} - x_n) \tag{17}$$

where, rand is a uniform distributed number within range [0, 1], and ρ_2 is a random parameter employed to modify step size of each vector agent. The ρ_2 parameter considers of significant parameters of the GBO exploration process. The ρ_2 parameter is computed as follows:

$$\rho_2 = 2 \times rand \times \alpha - \alpha. \tag{18}$$

Finally, depending on these terms GSR and DM, Eq.(19) and Eq.(20) are used to update the current vector (x_n^m) position.

$$X1_n^m = x_n^m - GSR + DM \tag{19}$$

where, $X1_n^m$is the new vector generated by updating x_n^m. According to Eq.(12) and Eq.(17), the $X1_n^m$ can be reformulated as:

$$X1_n^m = x_n^m - randn \times \rho_1 \times \frac{2\Delta x \times x_n^m}{(yp_n^m - yq_n^m + \varepsilon)} + randn \times \rho_2 \times \left(x_{\text{best}} - x_n^m\right) \tag{20}$$

where yp_n^m, yq_n^m are equal to $y_n + \Delta x$, and the $y_n - \Delta x$, y_n vector is equal to the average of the two vectors: current solution x_n and z_{n+1} vector. This is calculated as follows:

$$z_{n+1} = x_n - randn \times \frac{2\Delta x \times x_n}{(x_{\text{worst}} - x_{\text{best}} + \varepsilon)} \tag{21}$$

while x_n represents the current solution vector, *randn* is a random solution vector of dimension n, x_{worst} and x_{best} represent worst and best solutions, and Δx is given by Eq.(14). Based on the previous formula, when replacing the best solution vector x_{best} with the current solution vector x_n^m we get $X2_n^m$ the follows:

$$X2_n^m = x_{\text{best}} - randn \times \rho_1 \times \frac{2\Delta x \times x_n^m}{(yp_n^m - yq_n^m + \varepsilon)} + randn \times \rho_2 \times \left(x_{r1}^m - x_{r2}^m\right) \tag{22}$$

The GBO algorithm aims to enhance exploration and exploitation phases using Eq.(20) to improve the global search during the exploration phase, while Eq.(22) is used to improve the local search capability on exploitation phase. Finally, the new solution for the next iteration is generated as follows:

$$x_n^{m+1} = r_a \times \left(r_b \times X1_n^m + (1 - r_b) \times X2_n^m\right) + (1 - r_a) \times X3_n^m \tag{23}$$

where r_a, and r_b are random numbers determined in range [0, 1], and $X3_n^m$ is defined as:

$$X3_n^m = X_n^{m+1} - \rho 1 \times (X2_n^m - X1_n^m) \tag{24}$$

C. LOCAL ESCAPING OPERATOR STAGE

The Local Escaping operator (LEO) is introduced to strengthen the performance of an optimization algorithm for solving complex problems. The LEO can effectively update the position of the solution. Hence, it assists an algorithm to get out of local optima points, and speed the convergence. The LEO uses targets to generate a new solution with superior performance (X_{LEO}^m) several solutions (X_{best} best solution, the solutions $X1_n^m, X1_n^m$ are randomly selected from population, $X_{r1}^m, X1_{r2}^m$ randomly generated solutions). It effectively updates current solutions and the process is performed based on following scheme:

If rand < pr

$$X_{LEO}^m = \begin{cases} X_n^{m+1} + f_1\left(u_1 x_{\text{best}} - u_2 x_k^m\right) \\ \quad + f_2 \rho_1 \left(u_3 \left(X2_n^m - X1_n^m\right)\right) \\ \quad + u_2 \left(x_{r1}^m - x_{r2}^m\right)/2, & \text{if rand} < 0.5 \\ X_n^{m+1} + f_1\left(u_1 x_{\text{best}} - u_2 x_k^m\right) \\ \quad + f_2 \rho_1 \left(u_3 \left(X2_n^m - X1_n^m\right)\right) \\ \quad + u_2 \left(x_{r1}^m - x_{r2}^m\right)/2, & \text{otherwise} \end{cases} \tag{25}$$

End

where pr is a probability value, $pr = 0.5$, the values f_1, and f_2 are uniform distributed random numbers $\in [-1, 1]$, and u_1, u_2, u_3 are random values generated as following:

$$u_1 = \begin{cases} 2 \times \text{rand} & \text{if } \mu_1 < 0.5 \\ 1 & \text{otherwise} \end{cases} \tag{26}$$

$$u_2 = \begin{cases} \text{rand} & \text{if } \mu_1 < 0.5 \\ 1 & \text{otherwise} \end{cases} \tag{27}$$

$$u_3 = \begin{cases} \text{rand} & \text{if } \mu_1 < 0.5 \\ 1 & \text{otherwise} \end{cases} \tag{28}$$

where *rand* represents a random number $\in [0, 1]$, and μ_1 is a number in range [0, 1]. The previous equations for u_1, u_2, u_3, can be simply explained as follows:

$$u_1 = L_1 \times 2 \times rand + (1 - L_1) \tag{29}$$

$$u_2 = L_1 \times rand + (1 - L_1) \tag{30}$$

$$u_3 = L_1 \times rand + (1 - L_1) \tag{31}$$

where L_1 is a binary parameter takes value 0, 1, if parameter $\mu_1 < 0.5$, then value of $L_1 = 1$, otherwise $L_1 = 0$. The solution x_k^m is generated as follows:

$$x_k^m = \begin{cases} x_{\text{rand}} & \text{if } \mu_2 < 0.5 \\ x_p^m & \text{otherwise} \end{cases} \tag{32}$$

x_{rand} is a random generated solution according to following formula:

$$x_{\text{rand}} = X_{\min} + \text{rand}(0, 1) \times (X_{\max} - X_{\min}) \tag{33}$$

Algorithm 1 The Pseudo Code of the Gradient-Based Optimizer

Step 1. Initialization
Assign values for parameters pr, ε, M
Generate an initial population $X_0 = [x_{0,1}, x_{0,2}, \ldots, x_{o,D}]$
Evaluate the objective function value $f(X_0) =,\ n = 1, \ldots, N$
Specify the best and worst solutions x^m_{best} *and* x^m_{worst}
Step 2. Main loop
while $m < M$ **do**
  for $n = 1$ to N **do**
    for $n = 1$ to D **do**
      Select randomly $r1 \neq r2 \neq r3 \neq r4 \neq n$ in the range of $[1, N]$
      Calculate the position $x^{m+1}_{n,i}$ using Eq. (23)
    end for
    if rand$<$ pr **then** ▷ Local escaping operator
      Calculate the position x^m_{LEO} using Eq. (25)
      $x^{m+1}_n = x^m_{LEO}$
    end if
    Update the positions x^m_{best} and x^m_{worst}
  end for
  $m = m + 1$
end while
Step 2. Return x^m_{best}

x^m_p is a random selected solution from population and μ_2 is a random number $\in [0, 1]$.

Algorithm 1 describes the details pseudo-code of GBO algorithm.

V. ANALYSIS OF RESULTS

For fair benchmarking comparison, the GBO algorithm and the competitive algorithms have been tested with 30 independent runs and pr is set to 0.5 (default value). As demonstrated in [65], setting algorithm parameters to their default values is a fair and appropriate practice.

This section presents the analysis of the parameters extracted by the proposed GBO algorithm for various PV models. The objective function is optimized by the GBO. Other interesting approaches are also used for this problem, for example, the moth flame optimization (MFO) algorithm and cuckoo search algorithm (CSA). The performance of GBO was validated by the comparison of its results with other algorithms from previous work and with the CSA and MFO. In the following section, the primary discussion drawn from this study will be presented as well as the details of the extracted parameters, and the best RMSE by algorithms is performed.

The reported results are divided into three terms: the first data is the extracted parameters of each optimization algorithm at the best objective function (root mean square error); the second is the value of the simulated current and power at the parameters that achieve the best objective function extracted from the proposed GBO; then, based on the simulated current and power and the experimental power and current data, the absolute error for current data and the absolute error for power data are calculated; and the final data is the statistical analysis (minimum RMSE, mean of RMSE, maximum RMSE and standard deviation of RMSE) of the results extracted from all algorithms. These results are calculated for the SDM, DDM, and TDM.

A. RESULTS USING THE SINGLE-DIODE MODEL

The comparison of the results for SDM is presented in Table 2. This table includes the best RMSE and the parameters extracted from each algorithm. Based on the output data in Table 2, the RMSE of value 7.7301E-04 is achieved by COA and the best value of RMSE (9.8602E-4) was achieved by the GBO algorithm, together with ISCA, NMSOLMFO, ITLBO and MLBSA. While the second best RMSE (9.8607E-4) was achieved by GWOCS, followed by MFO, CSA, JAYA, LCJAYA and GWO respectively. The accuracy of the parameter values was measured by the RMSE. The absolute error (AE) for each value of power and current between the simulated and measured data was performed to evaluate the quality of the results shown in Table 3. The maximum value of AE for power was 1.462574E-03 and this current was less than 2.5085074E-03. The values of RMSE and AE for current and power confirm the quality and accuracy of the extracted parameters. The P-V and I-V curves for the SDM were based on the estimated data from the GBO at the best RMSE which is explained in Figure 4. In this figure, the proposed GBO was validated by comparing the simulation result with the experimental data of the R.T.C France solar cell. From this figure, it was observed that the simulation data output from the proposed GBO for SDM aligned with the measured data. So, the performance of the SDM based on GBO algorithm was more efficient.

TABLE 2. The parameters estimated for single diode model at the best root mean square error (RMSE).

Algorithm	$I_{ph}(A)$	$I_{s1}(\mu A)$	a_1	$R_s(\Omega)$	$R_{sh}(\Omega)$	RMSE
GBO	0.76077553	0.32302	1.481183596	0.036377092	53.71852549	9.8602E-04
MFO	0.760796012	0.3086	1.476593356	0.036557977	52.50655869	0.000989856
CSA	0.760892912	3.18E-07	1.479628661	0.036455939	52.44667219	0.000991184
MLBSA [26]	0.7608	0.323	1.4812	0.0364	53.7185	9.8600
MLBSA [26]	0.7608	0.323	1.4812	0.0364	53.7185	9.8602E-04
GWOCS [27]	0.760773	0.32192	1.4808	0.03639	53.632	9.8607E-04
GWO [27]	0.769969	0.91215	1.596658	0.02928	18.103	7.5011E-03
ISCA [28]	0.76077562	0.323017	1.4811822	0.03637716	53.71821748	9.8602E-04
LCJAYA [29]	0.7608	0.323	1.4819	0.0364	53.7185	0.00476841937654
JAYA [29]	0.7608	0.3281	1.4828	0.0364	54.9298	0.00255675552142
COA [31]	0.760788	0.31069	1.47727	0.03655	52.8898	7.7301E-04
ITLBO [33]	0.7608	0.323	1.4812	0.0364	53.7185	9.8602E-04

TABLE 3. Absolute error (AE) of single diode model at the best root mean square error using gradient-based optimizer.

Items	Real data		current simulated data		power simulated data	
	V(V)	$I_{exp}(A)$	$I_{sim}(A)$	$AE_I(A)$	$P_{sim}(w)$	$AE_P(w)$
1	-0.2057	0.764	0.764087704	8.77037E-05	-0.157172841	1.80407E-05
2	-0.1291	0.762	0.762663086	0.000663086	-0.098459804	8.56044E-05
3	-0.0588	0.7605	0.761355307	0.000855307	-0.044767692	5.02921E-05
4	0.0057	0.7605	0.760153991	0.000346009	0.004332878	1.97225E-06
5	0.0646	0.76	0.759055209	0.000944791	0.049034966	6.10335E-05
6	0.1185	0.759	0.758042345	0.000957655	0.089828018	0.000113482
7	0.1678	0.757	0.757091654	9.16539E-05	0.12703998	1.53795E-05
8	0.2132	0.757	0.756141365	0.000858635	0.161209339	0.000183061
9	0.2545	0.7555	0.755086873	0.000413127	0.192169609	0.000105141
10	0.2924	0.754	0.753663878	0.000336122	0.220371318	9.8282E-05
11	0.3269	0.7505	0.751390967	0.000890967	0.245629707	0.000291257
12	0.3585	0.7465	0.747353851	0.000853851	0.267926356	0.000306106
13	0.3873	0.7385	0.740117222	0.001617222	0.2866474	0.00062635
14	0.4137	0.728	0.727382225	0.000617775	0.300918027	0.000255573
15	0.4373	0.7065	0.706972651	0.000472651	0.30915914	0.00020669
16	0.459	0.6755	0.675280151	0.000219849	0.30995359	0.00010091
17	0.4784	0.632	0.630758272	0.001241728	0.301754758	0.000594042
18	0.496	0.573	0.571928358	0.001071642	0.283676466	0.000531534
19	0.5119	0.499	0.499607019	0.000607019	0.255748833	0.000310733
20	0.5265	0.413	0.413648792	0.000648792	0.217786089	0.000341589
21	0.5398	0.3165	0.31751011	0.00101011	0.171391957	0.000545257
22	0.5521	0.212	0.21215494	0.00015494	0.117130742	8.55421E-05
23	0.5633	0.1035	0.102251312	0.001248688	0.057598164	0.000703386
24	0.5736	-0.01	-0.008717541	0.001282459	-0.005000382	0.000735618
25	0.5833	-0.123	-0.125507413	0.002507413	-0.073208474	0.001462574
26	0.59	-0.21	-0.208472327	0.001527673	-0.122998673	0.000901327

B. RESULTS USING THE DOUBLE-DIODE MODEL

A comparative study of the results based on the DDM was introduced in Table 4. It includes the parameters extracted from each algorithm at the best RMSE. The results in Table 4, the best RMSE value (9.8237E-4) was achieved by ISCA algorithm, and the second best RMSE (9.8249E-4) was achieved by ITLBO together nearly with MLBSA. The third best RMSE (9.8258E-4) was computed from the GBO algorithm, followed by GWOCS, MFO, CSA, GWO, JAYA and LCJAYA, respectively. As for the SDM, the accuracy of the parameters was evaluated from the RMSE. The absolute error (AE) was also used for the current and power values in a comparison between the measured data presented in Table 5. The value of the AE for power was less than 1.48807E-03 and the maximum value of AE for current was 2.55113E-03. The values of RMSE and AE for current and power confirmed the quality and accuracy of the estimated parameters. The P-V and I-V curves for the DDM was based on the estimated data from GBO at the best RMSE, as explained in Figure 5. In this figure, the proposed GBO was validated by comparing the simulation result with the experimental data of R.T.C France solar cell. From this figure, it was observed that the simulation data output from the proposed GBO for double diode model aligned with the measured data. Thus, the performance of the DDM based on the GBO algorithm was more efficient.

C. RESULTS USING THE THREE-DIODE MODEL

A comparative study of the results based on the TDM is introduced in Table 6. The table shows the best RMSE and the parameters extracted from each algorithm. From Table 6, the optimal RMSE value (9.8249E-4) was achieved from the OBWOA algorithm, and the second best RMSE (9.82503E-4)

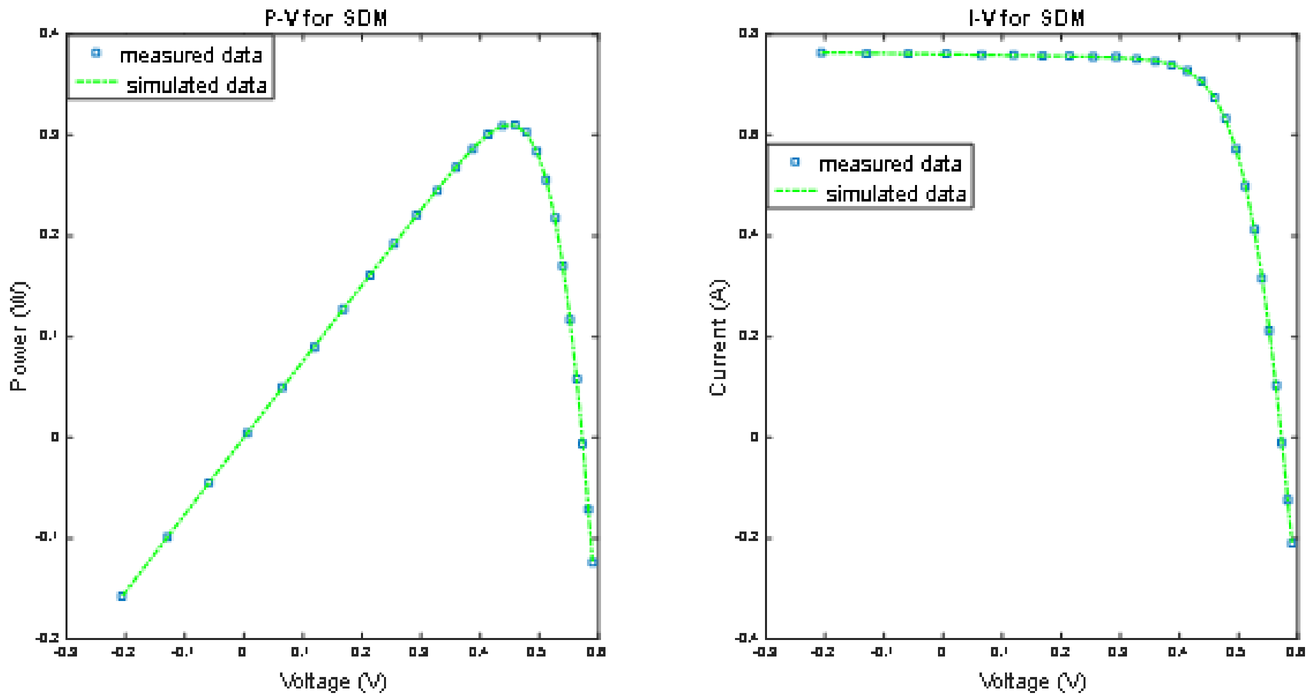

FIGURE 4. P-V and I-V curves for single diode model based on parameters extracted from gradient based optimizer.

TABLE 4. The parameters estimated of a double diode model at the best RMSE.

Algorithm	$I_{ph}(A)$	$I_{s1}(\mu A)$	a_1	$R_s(\Omega)$	$R_{sh}(\Omega)$	$I_{s2}(\mu A)$	a_2	RMSE
GBO	0.760780326	0.85705	1.999776183	0.036793056	55.7767015	0.2138	1.446432096	0.00098258
MFO	0.760843583	0.15736	1.421450251	0.037341537	52.92204541	0.7311	1.884225056	0.001007522
CSA	0.761759863	0.17618	1.429484164	0.037192705	46.45538652	0.96678	1.984563559	0.001123499
MLBSA [26]	0.7608	0.2273	1.4515	0.0367	55.4612	0.7384	2	0.00098249
GWOCS [27]	0.76076	0.53772	2	0.03666	54.7331	0.24855	1.4588	0.00098334
GWO [27]	0.761668	0.40302	1.646	0.03265	72.52775	0.45338	1.5527	0.0022124
ISCA [28]	0.760781079	0.7493463	2	0.036740424	55.48542959	0.22597411	1.4510169	0.00098237
LCJAYA [29]	0.7608	0.22596	1.4518	0.0367	55.4815	0.7464	2	0.00503457049
JAYA [29]	0.7607	0.0060763	1.8436	0.0364	52.6575	0.31507	1.4788	0.00227494479
COA [31]	0.76081	0.08656	1.37278	0.03803	52.3562	0.21597	2	7.3265E-04
ITLBO [33]	0.7608	0.226	1.451	0.0367	55.4854	0.7493	2	0.00098248

was achieved from the GBO, followed by STLBO, CIABS, MFO and CSA, respectively. Regarding the accuracy of the parameters obtained, RMSE was used as a proper metric. The AE was also used to verify the similarity between the simulated data and the measured data of the same data set used in Table 7. The value of AE for power was less than 1.485E-03 and the maximum value of AE for the current was 2.54586E-03. The values of RMSE and AE for the current and power confirmed the quality and accuracy of the extracted parameters. The P-V and I-V curves for the TDM were based on the estimated data from GBO at the best RMSE, as explained in Figure 6. In this figure, the proposed GBO was validated by comparing the simulation result with the experimental data of the R.T.C France solar cell. From this figure, it was observed that the simulation data output from the proposed GBO for three diode model aligned with the measured data. Thus, the performance of the TDM based on the GBO algorithm was more efficient.

D. STATISTICAL ANALYSIS

The accuracy and performance of all used algorithms are evaluated in this subsection. This evaluation was based on the values of RMSE for 30 independent runs of each algorithm. Table 8 shows the statistical analysis for each algorithm in all three PV models. The accuracy of an algorithm is indicated by the minimum value of RMSE, whereas the mean accuracy is reflected by the average RMSE, and the reliability of the system is reflected by the standard deviation (SD). Based on the results presented in Table 8, it was observed that the proposed GBO, MLBSA, LCJAYA, and ITLBO achieved the best accuracy and reliability in the SDM. The proposed GBO achieved the second-best accuracy in the DDM. Meanwhile,

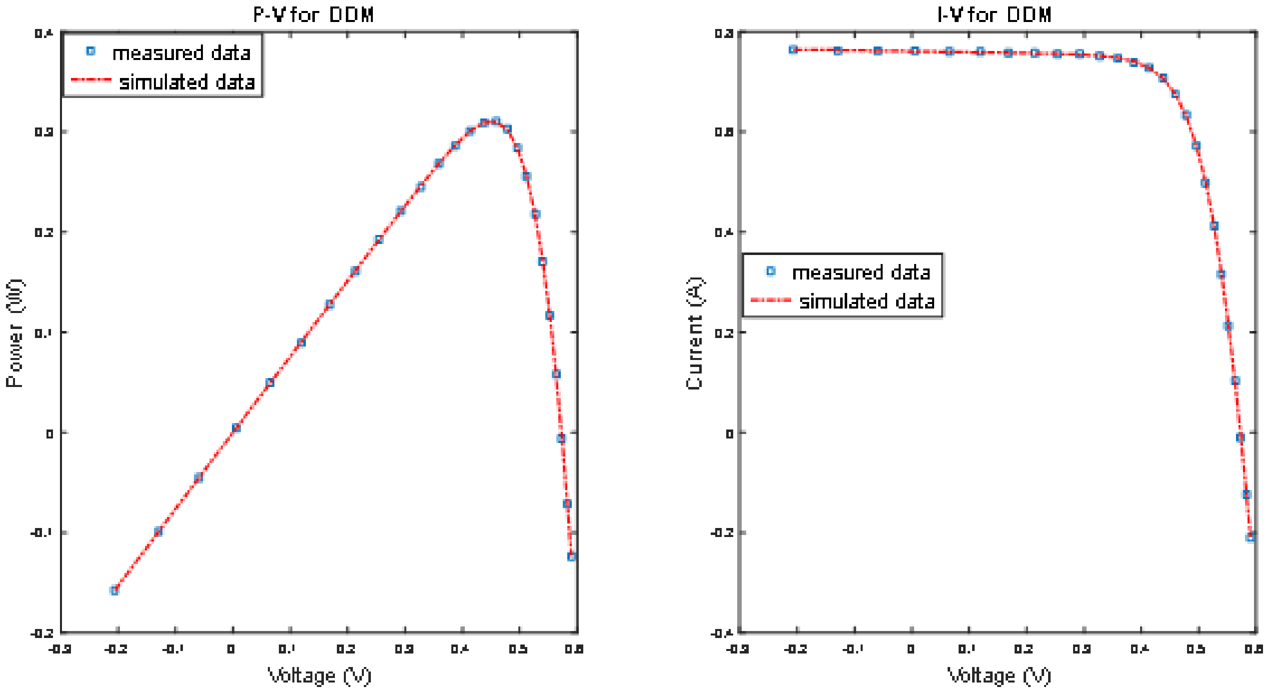

FIGURE 5. P-V and I-V curves for double diode model based on parameters extracted from gradient-based optimizer.

TABLE 5. Absolute error (AE) of double diode model at the best RMSE using gradient-based optimizer.

Current simulated data		Power simulated data	
$I_{sim}(A)$	$AE_I(A)$	$P_{sim}(w)$	$AE_P(w)$
0.763965313	3.46867E-05	-0.157147665	7.13506E-06
0.76259319	0.00059319	-0.098450781	7.65808E-05
0.761333364	0.000833364	-0.044766402	4.90018E-05
0.760175401	0.000324599	0.004333	1.85021E-06
0.759114502	0.000885498	0.049038797	5.72032E-05
0.758132509	0.000867491	0.089838702	0.000102798
0.75720262	0.00020262	0.1270586	3.39996E-05
0.756258569	0.000741431	0.161234327	0.000158073
0.755190525	0.000309475	0.192195989	7.87613E-05
0.753730606	0.000269394	0.220390829	7.87709E-05
0.751399367	0.000899367	0.245632453	0.000294003
0.74729178	0.00079178	0.267904103	0.000283853
0.739991809	0.001491809	0.286598828	0.000577778
0.727222708	0.000777292	0.300852034	0.000321566
0.706827301	0.000327301	0.309095579	0.000143129
0.675195557	0.000304443	0.309914761	0.000139739
0.630757708	0.001242292	0.301754487	0.000594313
0.572003297	0.000996703	0.283713635	0.000494365
0.499722096	0.000722096	0.255807741	0.000369641
0.413749921	0.000749921	0.217839333	0.000394833
0.31755683	0.00105683	0.171417177	0.000570477
0.21212393	0.00012393	0.117113622	6.84219E-05
0.102154801	0.001345199	0.0575438	0.00075775
-0.008800848	0.001199152	-0.005048167	0.000687833
-0.125551133	0.002551133	-0.073233976	0.001488076
-0.208363083	0.001636917	-0.122934219	0.000965781

the proposed GBO achieved the best accuracy and reliability in TDM.

E. ANALYSIS OF CONVERGENCE AND ROBUSTNESS

To graphically illustrate the robustness of the GBO against other algorithms, the convergence curves and robustness analysis are presented in this section. Figures 7, 8 and 9 explain the robustness and convergence curves of GBO, MFO, and CSA for the SDM, DDM, and TDM, respectively. The reliable robustness and faster convergence from these figures were from the GBO algorithm. The GBO reached a stable point for all PV models, and this behavior suggests that the GBO has good convergence capabilities. Figures 7, 8 and 9 show the convergence curves of all optimization algorithms for determining the parameters of PV modules for single, double, and three diode models, respectively. It was shown that the proposed algorithm (GBO) was the best one because it reached the minimum (best) value of the RMSE while the remaining algorithms did not reach to the best value of RMSE as the GBO.

In summary, the experimental results provided the following:

- The promising results obtained using the SDM, DDM, and TDM strongly prove that the GBO algorithm performs well in terms of RMSE, AE, and convergence and led to the optimal solutions shown in Sections V-D and V-E.
- The GBO algorithm showed superiority compared to the other algorithms in terms of RMSE, as shown in Table 2, 4 and 6.
- The GBO algorithm outperforms the other algorithms in term of AE, as shown in Tables 3, 5 and 7.
- The convergence curves and robustness behavior presented in Figures 7, 8 and 9 revealed that the GBO algorithm has better exploration and exploitation abilities than the other algorithms.

Overall, the solution extracted from the GBO converged to the global optima solution, and there were terms to determine

TABLE 6. The parameters estimated for three diode model at the best RMSE.

Algorithm	GBO	MFO	CSA	STLBO [36]	OBWOA [37]	CIABS [38]
$I_{ph}(A)$	0.760776979	7.61E-01	0.760358849	0.7608	0.76077	0.7607
$I_{s1}(\mu A)$	0.78129	0.42389	0	0.2349	0.2353	0.2
a_1	1.999994539	1.65E+00	1.826602665	1.44541	1.4543	1.4414
$R_s(\Omega)$	0.036758301	0.037131537	0.036699785	0.0367	0.03668	0.03687
$R_{sh}(\Omega)$	55.62330625	53.31146589	58.93317382	55.2641	55.4448	55.8344
$I_{s2}(\mu)$	0.221556	0.08147	0.15567	0.2297	0.2213	0.5
a_2	1.449384849	1.390944125	2	2	2	1.9
$I_{s3}(\mu A)$	0.00721	0.01843	0.2912	0.4443	0.4573	0.21
a_3	1.975652602	1.466698272	1.471740942	2	2	2
RMSE	0.000982503	0.000997027	0.001037665	9.8253E-04	9.8249E-04	9.8466E-04

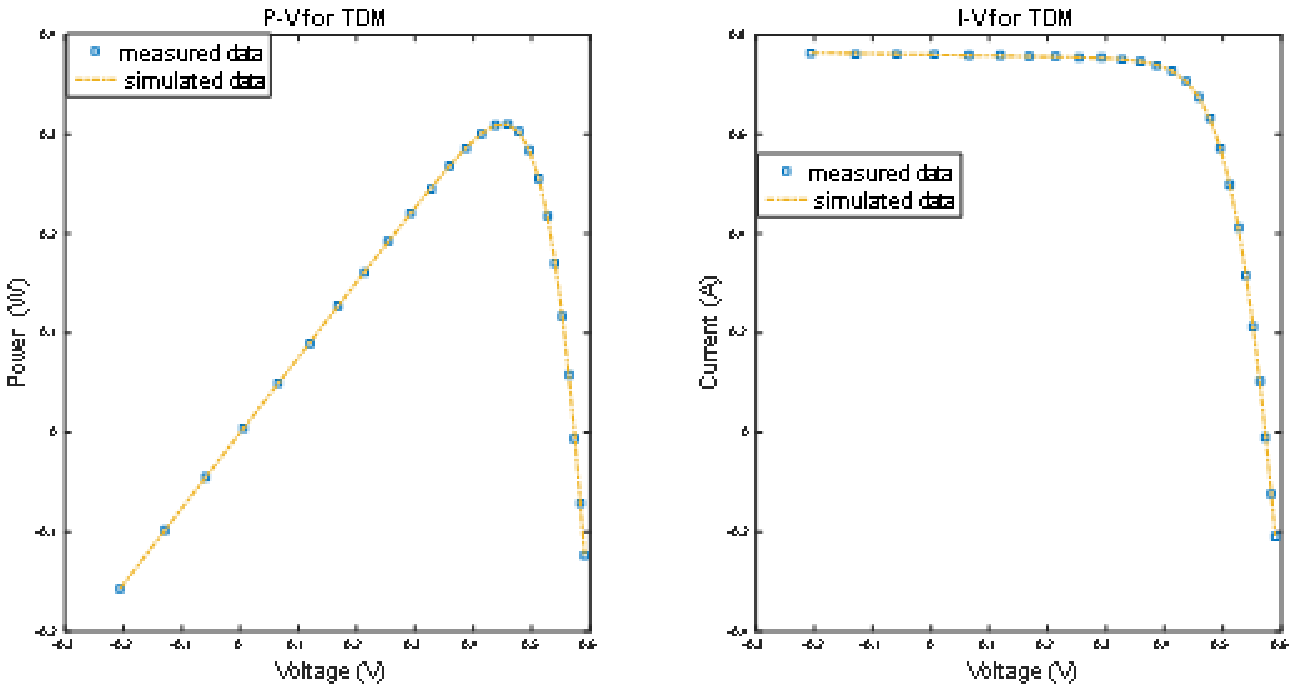

FIGURE 6. P-V and I-V curves for three diode model based on parameters extracted from gradient-based optimizer.

the quality of the solution. These terms were the mean and standard deviation for the 30 independent runs of the algorithms. Based on these runs, the robustness of the optimum solution was drawing like in Figures 7, 8, 9. From these figures, it was observed that the optimum solution for each run in nearly to each other over than other algorithms. The value of the standard deviation for the SDM was 1.7E-10. This value was indicated by all solutions of all runs and was approximately equal. Thus, the optimum solution of the GBO algorithm was converging to the global optima.

F. DISCUSSION

The purpose of this study is to propose an efficient search mechanism for optimizing the unknown's parameters of PV models. The experimental analysis and comparative study performed in earlier section suggest that proved the efficacy of GBO compared to the counterparts. The GBO algorithm presents certain advantages:

- The GBO is well able to perform an efficient search on the optimization landscapes that maintain varying difficulties and complexities. The GBO generates optimization solution with better fitness values than original and various other competitor methods. See Tables 2, 4, and 6.
- Also, in terms of Absolute error (AE), the GBO obtained the best AE values for each value of power and current between the simulated and measured data is performed to evaluate the results quality as shown in Tables 3, 5, and 7.
- Statistically, the optimization solutions generated by the GBO are significantly different than the ones generated by the various other optimization methods.
- The design of GBO is simple. Therefore, any opportunity to further enhance the algorithm is easy to implement.

TABLE 7. **(AE) Absolute error of three diode model at the best root mean square error using gradient-based optimizer.**

Current simulated data		Power simulated data	
$I_{sim}(A)$	$AE_I(A)$	$P_{sim}(w)$	$AE_P(w)$
0.763971166	2.88345E-05	-0.157148869	5.93125E-06
0.762595264	0.000595264	-0.098451049	7.68486E-05
0.76133199	0.00083199	-0.044766321	4.8921E-05
0.760170916	0.000329084	0.004332974	1.87578E-06
0.759107317	0.000892683	0.049038333	5.76673E-05
0.758123169	0.000876831	0.089837596	0.000103904
0.757191932	0.000191932	0.127056806	3.22062E-05
0.75624773	0.00075227	0.161232016	0.000160384
0.755181181	0.000318819	0.192193611	8.11394E-05
0.753724729	0.000275271	0.220389111	8.04892E-05
0.751398776	0.000898776	0.24563226	0.00029381
0.747297507	0.000797507	0.267906156	0.000285906
0.740003203	0.001503203	0.28660324	0.00058219
0.727237139	0.000762861	0.300858004	0.000315596
0.706840388	0.000340388	0.309101302	0.000148852
0.675202941	0.000297059	0.30991815	0.00013635
0.630757017	0.001242983	0.301754157	0.000594643
0.571994999	0.001005001	0.28370952	0.00049848
0.499709205	0.000709205	0.255801142	0.000363042
0.413737299	0.000737299	0.217832688	0.000388188
0.317548455	0.001048455	0.171412656	0.000565956
0.212122489	0.000122489	0.117112826	6.76263E-05
0.102160033	0.001339967	0.057546746	0.000754804
-0.008794868	0.001205132	-0.005044736	0.000691264
-0.125545865	0.002545865	-0.073230903	0.001485003
-0.20836846	0.00163154	-0.122937391	0.000962609

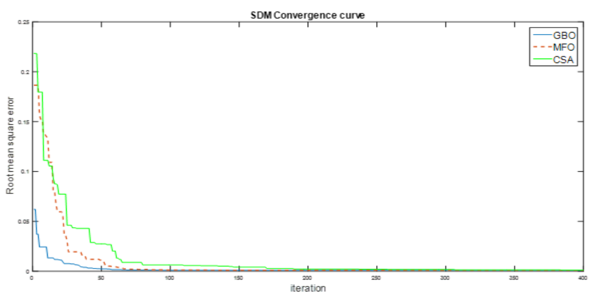

(a) The convergence curve for single diode model

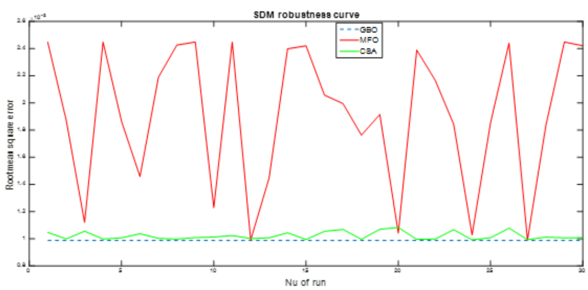

(b) The robustness curve for the single diode model

FIGURE 7. **The convergence and robustness curves for single diode model.**

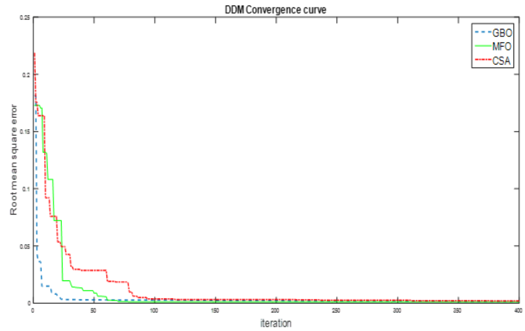

(a) The convergence curve for the double diode model.

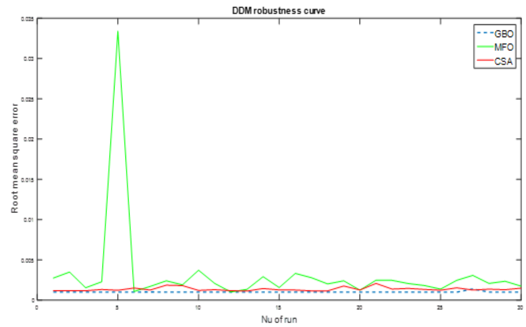

(b) The robustness curve for the double diode model.

FIGURE 8. **The convergence and robustness curves for the double diode model.**

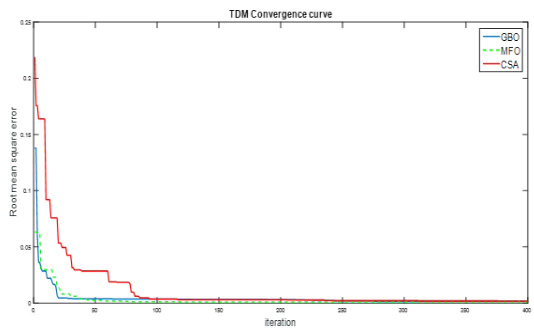

(a) The convergence curve for the three diode model.

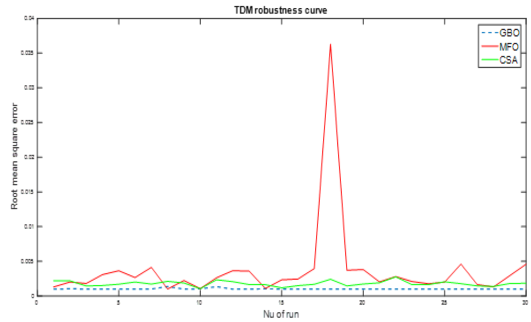

(b) The robustness curve for the three diode model.

FIGURE 9. **The convergence and robustness curves for the three diode model.**

Besides benefits, the GBO also poses some limitations as discussed below:

- In this GBO, ρ_1 is introduced as the most significant parameter in the GBO to balance the exploration and exploitation searching processes. Thus modification in this parameter deems tricky when employed on optimization problems with difficult problem landscapes

TABLE 8. Statistical analysis of root mean square error for three photovoltaic models.

Model	Algorithm	RMSE			
		Min	Max	Average	SD
SDM	GBO	9.8602E-04	9.8602E-04	9.8602E-04	1.753E-10
	MFO	0.000989856	0.002448049	0.001912964	5.22926E-04
	CSA	9.91184E-04	1.081737E-03	1.021315E-03	2.94913E-05
	GWOCS [27]	9.8607E-04	9.9095E-04	9.8874E-04	2.4696E-06
	GWO [27]	7.5011E-03	3.8160E-02	2.5617-02	1.6071E-02
	ISCA [28]	7.34231E-04	7.45921E-04	7.23043E-04	1.30287E-06
	LCJAYA [29]	9.86E-04	9.86E-04	9.86E-04	5.70E-16
	JAYA [29]	9.8946E-04	1.4783E-03	1.1617E-03	1.8796E-04
	ITLBO [33]	9.8602E-04	9.8602E-04	9.8602E-04	2.19E-17
	MLBSA [26]	9.8602-04	9.8602E-04	9.8602 E-04	9.15E-12
DDM	GBO	9.825797E-04	1.00054E-03	1.38203E-03	7.231E-05
	MFO	1.00752E-03	3.34096E-02	3.21918E-03	5.74432E-03
	CSA	1.12349E-03	2.07298E-03	1.35984E-03	2.366E-04
	GWOCS [27]	9.8334E-04	1.0017E-03	9.9411E-04	9.5937E-06
	GWO [27]	2.2124E-03	3.7996E-02	1.6222E-02	1.9113E-02
	ISCA [28]	9.8342E-04	9.86863E-04	9.83800E-04	1.65397E-06
	LCJAYA [29]	9.83E-04	9.86E-04	9.83E-04	1.31E-06
	JAYA [29]	1.31E-06	1.4793E-03	1.1767E-03	1.9356E-04
	ITLBO [33]	9.8248E-04	9.8812E-04	9.8497E-04	1.54E-06
	MLBSA [26]	9.8249E-04	9.8249E-04	9.8518E-04	1.35E-06
TDM	GBO	9.82503E-04	1.3636E-03	9.84283E-04	9.391E-05
	MFO	9.97027E-04	3.62978E-02	3.7394E-03	6.2405E-03
	CSA	1.03766E-03	2.764015E-03	1.788847E-03	3.74083E-04

- The parameter α changes with the iteration number. It has a large value at the early iterations to enhance the population diversity and then its value decreases as the iteration number increases to accelerate the convergence, thus this dependent on the problem type.
- Because GBO is an optimization technique based on randomization, its selected values may vary every time it is run. Therefore, there is no guarantee that the values subset selected in one run can be found in another run, which may bring confusion for the end user.

VI. CONCLUSION AND FUTURE WORK

This paper presented a new application of the GBO to estimate the parameters of three PV models. The three models were SDM, DDM, and TDM. The main idea of this work was to efficiently design the three PV models from the proper estimation of their parameters. The single diode mathematical model was formulated as a nonlinear equation between the current and voltage, including five unknown parameters due to the manufacture datasheet's shortage of data. Also, the DDM and TDM operated like the SDM, except the number of unknown parameters in the DDM is seven and in TDM is nine. The objective function of the extracted parameters in the three PV model was minimizing the root mean square error between the simulated current and the experimental current of the R.T.C France solar cell. The proposed GBO is a recent optimization technique employed to minimize the objective function of the parameter extraction of PV cells by using the SDM, DDM, and TDM. The GBO algorithm has various advantages, such as solution accuracy, balance, and convergence speed between analysis and exploitation. The results achieved by the GBO were more accurate than those achieved by most of the ten competitor algorithms. The GBO is, thus, a good candidate for solving the optimization problems of solar cell systems. In future work, the GBO can be applied to identify the PV parameters multidimensional diode and models, and also for calculating the current voltage characteristics of multi-diode diodes and models.

CONFLICT OF INTEREST

The authors declare that there is no conflict of interest. Non-financial competing interests.

CREDIT AUTHOR STATEMENT

Alaa A. K. Ismaeel: Methodology, Formal analysis, Writing - review & editing. Essam H. Houssein: Supervision, Methodology, Conceptualization, Formal analysis, Writing - review & editing. Mokhtar Said: Software, Formal analysis, Resources, Writing - original draft. Diego Oliva: Conceptualization, Methodology, Formal analysis, Writing - review & editing. All authors read and approved the final paper.

REFERENCES

[1] M. F. AlHajri, K. M. El-Naggar, M. R. AlRashidi, and A. K. Al-Othman, "Optimal extraction of solar cell parameters using pattern search," *Renew. Energy*, vol. 44, pp. 238–245, Aug. 2012.

[2] J. Jurasz, F. A. Canales, A. Kies, M. Guezgouz, and A. Beluco, "A review on the complementarity of renewable energy sources: Concept, metrics, application and future research directions," *Sol. Energy*, vol. 195, pp. 703–724, Jan. 2020.

[3] I. Nassar-Eddine, A. Obbadi, Y. Errami, A. E. Fajri, and M. Agunaou, "Parameter estimation of photovoltaic modules using iterative method and the Lambert W function: A comparative study," *Energy Convers. Manage.*, vol. 119, pp. 37–48, Jul. 2016.

[4] H. M. Hasanien, "Performance improvement of photovoltaic power systems using an optimal control strategy based on whale optimization algorithm," *Electr. Power Syst. Res.*, vol. 157, pp. 168–176, Apr. 2018.

[5] B. Parida, S. Iniyan, and R. Goic, "A review of solar photovoltaic technologies," *Renew. Sustain. Energy Rev.*, vol. 15, no. 3, pp. 1625–1636, 2011.

[6] M. A. Mohamed, T. Jin, and W. Su, "An effective stochastic framework for smart coordinated operation of wind park and energy storage unit," *Appl. Energy*, vol. 272, Aug. 2020, Art. no. 115228.

[7] X. Gong, F. Dong, M. A. Mohamed, E. M. Awwad, H. M. Abdullah, and Z. M. Ali, "Towards distributed based energy transaction in a clean smart island," *J. Cleaner Prod.*, vol. 273, Nov. 2020, Art. no. 122768.

[8] M. El-Negamy, M. Eteiba, and G. El-Bayoumi, "Modeling and simulation of Egyptsat-1 satellite system powered by photovoltaic module," *J. Amer. Sci.*, vol. 9, no. 1, pp. 110–116, 2013.

[9] M. Mostafa, H. M. Abdullah, and M. A. Mohamed, "Modeling and experimental investigation of solar stills for enhancing water desalination process," *IEEE Access*, vol. 8, pp. 219457–219472, 2020.

[10] S. Mahdavi, F. Sarhaddi, and M. Hedayatizadeh, "Energy/exergy based-evaluation of heating/cooling potential of PV/T and earth-air heat exchanger integration into a solar greenhouse," *Appl. Thermal Eng.*, vol. 149, pp. 996–1007, Feb. 2019.

[11] D. Kapoor, P. Sodhi, and D. Deb, "Solar panel simulation using adaptive control," in *Proc. IEEE Int. Conf. Control Appl.*, Oct. 2012, pp. 1124–1130.

[12] D. Kapoor, P. Sodhi, and D. Deb, "A novel control strategy to simulate solar panels," in *Proc. Int. Conf. Signal Process. Commun. (SPCOM)*, Jul. 2012, pp. 1–5.

[13] S. Mishra, K. Bhargava, and D. Deb, "Numerical simulation of potential induced degradation (PID) in different thin-film solar cells using SCAPS-1D," *Sol. Energy*, vol. 188, pp. 353–360, Aug. 2019.

[14] D. Deb and N. L. Brahmbhatt, "Review of yield increase of solar panels through soiling prevention, and a proposed water-free automated cleaning solution," *Renew. Sustain. Energy Rev.*, vol. 82, pp. 3306–3313, Feb. 2018.

[15] M. A. Soliman, H. M. Hasanien, and A. Alkuhayli, "Marine predators algorithm for parameters identification of triple-diode photovoltaic models," *IEEE Access*, vol. 8, pp. 155832–155842, 2020.

[16] O. S. Elazab, H. M. Hasanien, M. A. Elgendy, and A. M. Abdeen, "Parameters estimation of single-and multiple-diode photovoltaic model using whale optimisation algorithm," *IET Renew. Power Gener.*, vol. 12, no. 15, pp. 1755–1761, Nov. 2018.

[17] E. H. Houssein, Y. Mina, and E. Aboul, "Nature-inspired algorithms: A comprehensive review," in *Hybrid Computational Intelligence: Research and Applications*. Boca Raton, FL, USA: CRC Press, 2019, p. 1.

[18] M. Ei-Negamy, A. Galal, and G. Ei-Bayoumin, "Extraction of the unknown parameters of a photovoltaic module from manufacture data sheet," *Int. J. Innov. Sci. Mod. Eng.*, vol. 3, no. 10, pp. 6–13, Sep. 2015.

[19] J. Cubas, S. Pindado, and C. de Manuel, "Explicit expressions for solar panel equivalent circuit parameters based on analytical formulation and the Lambert W-function," *Energies*, vol. 7, no. 7, pp. 4098–4115, Jun. 2014.

[20] S. Madi and A. Kheldoun, "Bond graph based modeling for parameter identification of photovoltaic module," *Energy*, vol. 141, pp. 1456–1465, Dec. 2017.

[21] E. Cuce, P. M. Cuce, I. H. Karakas, and T. Bali, "An accurate model for photovoltaic (PV) modules to determine electrical characteristics and thermodynamic performance parameters," *Energy Convers. Manage.*, vol. 146, pp. 205–216, Aug. 2017.

[22] H. E. Achouby, M. Zaimi, A. Ibral, and E. M. Assaid, "New analytical approach for modelling effects of temperature and irradiance on physical parameters of photovoltaic solar module," *Energy Convers. Manage.*, vol. 177, pp. 258–271, Dec. 2018.

[23] F. J. Toledo, J. M. Blanes, and V. Galiano, "Two-step linear least-squares method for photovoltaic single-diode model parameters extraction," *IEEE Trans. Ind. Electron.*, vol. 65, no. 8, pp. 6301–6308, Aug. 2018.

[24] A. Chatterjee, A. Keyhani, and D. Kapoor, "Identification of photovoltaic source models," *IEEE Trans. Energy Convers.*, vol. 26, no. 3, pp. 883–889, Sep. 2011.

[25] B. Yang, J. Wang, X. Zhang, T. Yu, W. Yao, H. Shu, F. Zeng, and L. Sun, "Comprehensive overview of meta-heuristic algorithm applications on PV cell parameter identification," *Energy Convers. Manage.*, vol. 208, Mar. 2020, Art. no. 112595.

[26] K. Yu, J. J. Liang, B. Y. Qu, Z. Cheng, and H. Wang, "Multiple learning backtracking search algorithm for estimating parameters of photovoltaic models," *Appl. Energy*, vol. 226, pp. 408–422, Sep. 2018.

[27] W. Long, S. Cai, J. Jiao, M. Xu, and T. Wu, "A new hybrid algorithm based on grey wolf optimizer and cuckoo search for parameter extraction of solar photovoltaic models," *Energy Convers. Manage.*, vol. 203, Jan. 2020, Art. no. 112243.

[28] H. Chen, S. Jiao, A. A. Heidari, M. Wang, X. Chen, and X. Zhao, "An opposition-based sine cosine approach with local search for parameter estimation of photovoltaic models," *Energy Convers. Manage.*, vol. 195, pp. 927–942, Sep. 2019.

[29] X. Jian and Z. Weng, "A logistic chaotic JAYA algorithm for parameters identification of photovoltaic cell and module models," *Optik*, vol. 203, Feb. 2020, Art. no. 164041.

[30] G. Xiong, J. Zhang, D. Shi, L. Zhu, X. Yuan, and Z. Tan, "Winner-leading competitive swarm optimizer with dynamic Gaussian mutation for parameter extraction of solar photovoltaic models," *Energy Convers. Manage.*, vol. 206, Feb. 2020, Art. no. 112450.

[31] V. J. Chin and Z. Salam, "Coyote optimization algorithm for the parameter extraction of photovoltaic cells," *Sol. Energy*, vol. 194, pp. 656–670, Dec. 2019.

[32] H. Zhang, A. A. Heidari, M. Wang, L. Zhang, H. Chen, and C. Li, "Orthogonal Nelder–Mead moth flame method for parameters identification of photovoltaic modules," *Energy Convers. Manage.*, vol. 211, May 2020, Art. no. 112764.

[33] S. Li, W. Gong, X. Yan, C. Hu, D. Bai, L. Wang, and L. Gao, "Parameter extraction of photovoltaic models using an improved teaching-learning-based optimization," *Energy Convers. Manage.*, vol. 186, pp. 293–305, Apr. 2019.

[34] D. Allam, D. A. Yousri, and M. B. Eteiba, "Parameters extraction of the three diode model for the multi-crystalline solar cell/module using moth-flame optimization algorithm," *Energy Convers. Manage.*, vol. 123, pp. 535–548, Sep. 2016.

[35] R. Chenouard and R. A. El-Sehiemy, "An interval branch and bound global optimization algorithm for parameter estimation of three photovoltaic models," *Energy Convers. Manage.*, vol. 205, Feb. 2020, Art. no. 112400.

[36] Q. Niu, H. Zhang, and K. Li, "An improved TLBO with elite strategy for parameters identification of PEM fuel cell and solar cell models," *Int. J. Hydrogen Energy*, vol. 39, no. 8, pp. 3837–3854, Mar. 2014.

[37] M. A. Elaziz and D. Oliva, "Parameter estimation of solar cells diode models by an improved opposition-based whale optimization algorithm," *Energy Convers. Manage.*, vol. 171, pp. 1843–1859, Sep. 2018.

[38] D. Oliva, A. A. Ewees, M. A. E. Aziz, A. E. Hassanien, and M. Peréz-Cisneros, "A chaotic improved artificial bee colony for parameter estimation of photovoltaic cells," *Energies*, vol. 10, no. 7, p. 865, Jun. 2017.

[39] M. H. Qais, H. M. Hasanien, and S. Alghuwainem, "Parameters extraction of three-diode photovoltaic model using computation and Harris Hawks optimization," *Energy*, vol. 195, Mar. 2020, Art. no. 117040.

[40] J. A. Jervase, H. Bourdoucen, and A. Al-Lawati, "Solar cell parameter extraction using genetic algorithms," *Meas. Sci. Technol.*, vol. 12, no. 11, p. 1922, 2001.

[41] M. S. Ismail, M. Moghavvemi, and T. M. I. Mahlia, "Characterization of PV panel and global optimization of its model parameters using genetic algorithm," *Energy Convers. Manage.*, vol. 73, pp. 10–25, Sep. 2013.

[42] P. A. Kumari and P. Geethanjali, "Adaptive genetic algorithm based multi-objective optimization for photovoltaic cell design parameter extraction," *Energy Procedia*, vol. 117, pp. 432–441, Jun. 2017.

[43] K. Ishaque, Z. Salam, S. Mekhilef, and A. Shamsudin, "Parameter extraction of solar photovoltaic modules using penalty-based differential evolution," *Appl. Energy*, vol. 99, pp. 297–308, Nov. 2012.

[44] D. H. Muhsen, A. B. Ghazali, T. Khatib, and I. A. Abed, "Extraction of photovoltaic module model's parameters using an improved hybrid differential evolution/electromagnetism-like algorithm," *Sol. Energy*, vol. 119, pp. 286–297, Sep. 2015.

[45] N. Muangkote, K. Sunat, S. Chiewchanwattana, and S. Kaiwinit, "An advanced onlooker-ranking-based adaptive differential evolution to extract the parameters of solar cell models," *Renew. Energy*, vol. 134, pp. 1129–1147, Apr. 2019.

[46] A. Askarzadeh and A. Rezazadeh, "Artificial bee swarm optimization algorithm for parameters identification of solar cell models," *Appl. Energy*, vol. 102, pp. 943–949, Feb. 2013.

[47] Z. Wu, D. Yu, and X. Kang, "Parameter identification of photovoltaic cell model based on improved ant lion optimizer," *Energy Convers. Manage.*, vol. 151, pp. 107–115, Nov. 2017.

[48] R. Abbassi, A. Abbassi, A. A. Heidari, and S. Mirjalili, "An efficient salp swarm-inspired algorithm for parameters identification of photovoltaic cell models," *Energy Convers. Manage.*, vol. 179, pp. 362–372, Jan. 2019.

[49] A. Abbassi, R. Abbassi, A. A. Heidari, D. Oliva, H. Chen, A. Habib, M. Jemli, and M. Wang, "Parameters identification of photovoltaic cell models using enhanced exploratory salp chains-based approach," *Energy*, vol. 198, May 2020, Art. no. 117333.

[50] Q. Niu, L. Zhang, and K. Li, "A biogeography-based optimization algorithm with mutation strategies for model parameter estimation of solar and fuel cells," *Energy Convers. Manage.*, vol. 86, pp. 1173–1185, Oct. 2014.

[51] T. Kang, J. Yao, M. Jin, S. Yang, and T. Duong, "A novel improved cuckoo search algorithm for parameter estimation of photovoltaic (PV) models," *Energies*, vol. 11, no. 5, p. 1060, Apr. 2018.
[52] A. Askarzadeh and L. dos Santos Coelho, "Determination of photovoltaic modules parameters at different operating conditions using a novel bird mating optimizer approach," *Energy Convers. Manage.*, vol. 89, pp. 608–614, Jan. 2015.
[53] J. P. Ram, T. S. Babu, T. Dragicevic, and N. Rajasekar, "A new hybrid bee pollinator flower pollination algorithm for solar PV parameter estimation," *Energy Convers. Manage.*, vol. 135, pp. 463–476, Mar. 2017.
[54] M. A. Awadallah, "Variations of the bacterial foraging algorithm for the extraction of PV module parameters from nameplate data," *Energy Convers. Manage.*, vol. 113, pp. 312–320, Apr. 2016.
[55] B. Jacob, K. Balasubramanian, S. M. Azharuddin, and N. Rajasekar, "Solar PV modelling and parameter extraction using artificial immune system," *Energy Procedia*, vol. 75, pp. 331–336, Aug. 2015.
[56] H. M. Ridha, A. A. Heidari, M. Wang, and H. Chen, "Boosted mutation-based Harris Hawks optimizer for parameters identification of single-diode solar cell models," *Energy Convers. Manage.*, vol. 209, Apr. 2020, Art. no. 112660.
[57] H. M. Ridha, C. Gomes, and H. Hizam, "Estimation of photovoltaic module model's parameters using an improved electromagnetic-like algorithm," *Neural Comput. Appl.*, vol. 32, pp. 1–16, Jan. 2020.
[58] J. Montano, A. Tobón, J. P. Villegas, and M. Durango, "Grasshopper optimization algorithm for parameter estimation of photovoltaic modules based on the single diode model," *Int. J. Energy Environ. Eng.*, vol. 11, pp. 1–9, Feb. 2020.
[59] G. Xiong, J. Zhang, D. Shi, and Y. He, "Parameter extraction of solar photovoltaic models using an improved whale optimization algorithm," *Energy Convers. Manage.*, vol. 174, pp. 388–405, Oct. 2018.
[60] Y. Rao, Z. Shao, A. H. Ahangarnejad, E. Gholamalizadeh, and B. Sobhani, "Shark smell optimizer applied to identify the optimal parameters of the proton exchange membrane fuel cell model," *Energy Convers. Manage.*, vol. 182, pp. 1–8, Feb. 2019.
[61] D. H. Wolpert and W. G. Macready, "No free lunch theorems for optimization," *IEEE Trans. Evol. Comput.*, vol. 1, no. 1, pp. 67–82, Apr. 1997.
[62] I. Ahmadianfar, O. Bozorg-Haddad, and X. Chu, "Gradient-based optimizer: A new metaheuristic optimization algorithm," *Inf. Sci.*, vol. 540, pp. 131–159, Nov. 2020.
[63] D. Yousri, S. B. Thanikanti, D. Allam, V. K. Ramachandaramurthy, and M. B. Eteiba, "Fractional chaotic ensemble particle swarm optimizer for identifying the single, double, and three diode photovoltaic models' parameters," *Energy*, vol. 195, Mar. 2020, Art. no. 116979.
[64] I. A. Ibrahim, M. J. Hossain, B. C. Duck, and M. Nadarajah, "An improved wind driven optimization algorithm for parameters identification of a triple-diode photovoltaic cell model," *Energy Convers. Manage.*, vol. 213, Jun. 2020, Art. no. 112872.
[65] A. Arcuri and G. Fraser, "Parameter tuning or default values? An empirical investigation in search-based software engineering," *Empirical Softw. Eng.*, vol. 18, no. 3, pp. 594–623, Jun. 2013.

ALAA A. K. ISMAEEL received the B.S. degree in mathematics and computer science and the M.Sc. degree in computer science from Minia University, Egypt, in June 1998 and June 2004, respectively, and the Ph.D. degree in computer science "information visualization" from the Karlsruhe Institute of Technology-KIT, Germany, in May 2012. Since 2013, he has been working as an Assistant Professor with the Faculty of Computer Studies FCS, Arab Open University AOU, Oman. His research interests include optimization, dynamic graph drawing, efficient graph algorithms, computational geometry, information visualization, big data visualization, MANETs, routing protocols, and metaheuristic techniques.

ESSAM H. HOUSSEIN received the Ph.D. degree in computer science wireless networks based on artificial intelligence, in 2012. He is currently working as an Associate Professor with the Faculty of Computers and Information, Minia University, Egypt. He is also the Founder of the Computing and Artificial Intelligence Research Group (CAIRG), Egypt. He has more than 80 scientific research articles published in prestigious international journals in the topics of optimization, machine learning, image processing, the IoT, and its applications. His research interests include wireless sensor networks, the IoT, bioinformatics and biomedical, cloud computing, soft computing, image processing, artificial intelligence, data mining, optimization, and metaheuristics techniques. He serves as a Reviewer for more than 30 journals (Elsevier, Springer, and IEEE).

DIEGO OLIVA received the B.S. degree in electronics and computer engineering from the Industrial Technical Education Center (CETI) of Guadalajara, Mexico, in 2007, the M.Sc. degree in electronic engineering and computer sciences from the University of Guadalajara, Mexico, in 2010, and the Ph.D. degree in informatics from the Universidad Complutense de Madrid, in 2015. He is currently an Associate Professor with the University of Guadalajara, Mexico. His research interests include evolutionary and swarm algorithms, hybridization of evolutionary and swarm algorithms, and image processing.

MOKHTAR SAID received the B.Sc. degree (Hons.) in electrical engineering, the M.Sc. and Ph.D. degrees in renewable energy from the Faculty of Engineering, Fayoum University, Egypt, in June 2009, September 2013, and 2018, respectively. His research interests include modeling and simulation of electrical systems, electrical drives control, and optimization of renewable energy systems.